IL NUOVO CIMENTO Vol. 34 C, N. 5 Settembre-Ottobre 2011
DOI 10.1393/ncc/i2011-10926-6

Communications: SIF Congress 2010

Ti/Au TES as photon-number–resolving detector

L. Lolli

DISPEA, Politecnico di Torino - C.so Duca degli Abruzzi 24, 10129 Torino, Italy
Instituto Nazionale di Ricerca Metrologica INRIM - Strada delle Cacce 91
10135 Torino, Italy

(ricevuto il 31 Dicembre 2010; approvato il 24 Marzo 2011; pubblicato online il 2 Agosto 2011)

Summary. — One of the most promising detector, able to resolve single photons thanks to their intrinsic energy resolution, is the transition-edge sensor (TES). We present the state of the art on these superconducting single-photon detectors, developed and characterised at the National Institute of Metrological Research (INRIM). We show both the physical properties and the best results obtained on a Ti/Au TES in the spectral range between visible and near infrared.

PACS 29.40.Vj – Calorimeters.
PACS 42.50.Ar – Photon statistics and coherence theory.
PACS 85.25.Oj – Superconducting optical, X-ray, and γ-ray detectors (SIS, NIS, transition edge).
PACS 85.25.-j – Superconducting devices.

1. – Introduction

Single-photon detectors are fundamental devices in several scientific fields, like in optical science and technology [1]. For example, they play a crucial role in quantum information and computation to exploit quantum systems for the elaboration and communication of information, or in quantum-based metrology for the reformulation of the candela in terms of a quantum standard based on a fundamental constant [2] or for the absolute calibration of detectors [3].

A transition-edge sensor is a superconductive detector which works as a microcalorimeter taking advantage from its very sharp transition from superconducting to normal state. TESs are able to detect single photons from NIR to X-ray with an intrinsic energy resolution and photon number discrimination capability [4].

In the present work we present the electro-optic characterization of TiAu TESs. Thermal and electrical parameters, such as heat capacity, thermal conductance, logarithmic temperature sensitivity and the logarithmic current sensitivity, have been estimated using impedance measurements technique [5]. Photon number resolving capability, obtained by means of a new coupling system [6] and irradiating our devices at 690 nm, 1310 nm and 1570 nm, is also presented.

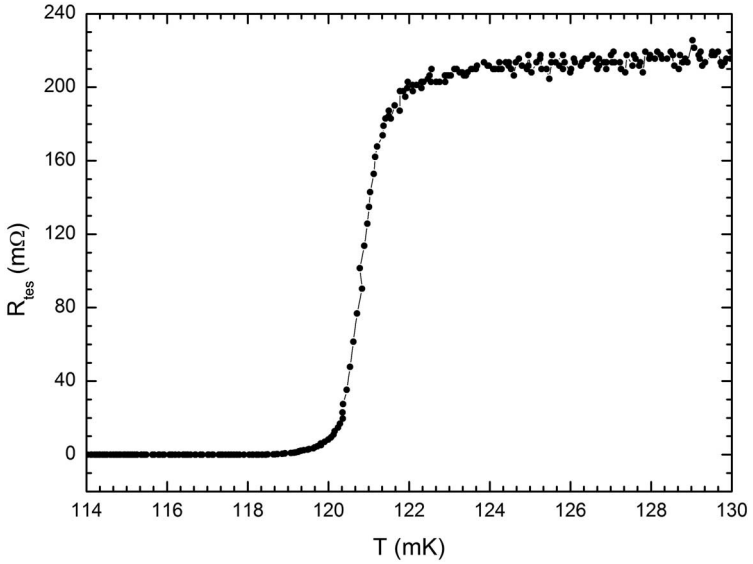

Fig. 1. – TES resistance *vs.* temperature for a TiAu bilayer with $T_c = 121\,\mathrm{mK}$, $\Delta T_c = 2\,\mathrm{mK}$ and $R_n = 0.220\,\Omega$.

2. – TESs characterization

At INRIM we fabricate and characterize TES detectors made by several kind of materials. In this manuscript we focus on devices based on TiAu bilayer films, with an overall thickness of about 80 nm and area of $20\,\mu\mathrm{m} \times 20\,\mu\mathrm{m}$ and $10\,\mu\mathrm{m} \times 10\,\mu\mathrm{m}$, respectively. More details on devices fabrication are reported in another paper [7].

The proximity effect between Ti and Au, combined with the thicknesses control, allows to obtain critical temperatures ranging from 80 mK to 130 mK, transition width of few mK and normal resistance (R_n) of hundreds of mΩ. The detector is voltage biased with a shunt resistance R_{sh} of 2.38 mΩ and read out using a DC-SQUID current sensor [8], whose input coil is in series with the TES [9].

The transition curve reported in fig. 1 corresponds to a $20\,\mu\mathrm{m} \times 20\,\mu\mathrm{m}$ TES, with $T_c = 121\,\mathrm{mK}$, $\Delta T_c = 2\,\mathrm{mK}$ and $R_n = 0.220\,\Omega$. It has been obtained with a constant sinusoidal current of $0.5\,\mu\mathrm{A}$ applied to the bias circuit. The polarization curve, reporting the current passing through the TES I_{tes} *vs.* the applied bias current I_{bias}, is shown in fig. 2, at fixed bath temperature of $\sim 39\,\mathrm{mK}$. The superconducting region is present for $I_{bias} < 40\,\mu\mathrm{A}$, while the normal region begins for $I_{bias} > 400\,\mu\mathrm{A}$, corresponding to 220 mΩ. The working point is chosen through the superconducting-to-normal transition region at $I_{bias} = 95\,\mu\mathrm{A}$ corresponding to 17 mΩ (about 8% of R_N).

For a complete characterisation of microcalorimeters it is necessary to evaluate their thermal and electrical properties. To this purpose the complex impedance measurement technique is an established and powerful method. The impedance of our TiAu TES is measured using the experimental set-up described in [5]. By fitting the experimental data to a suitable model [10], we obtain information about the logarithmic temperature sensitivity α, the logarithmic current sensitivity β and on the device thermal parameters, heat capacity C and thermal conductance G. The complex impedance measurements

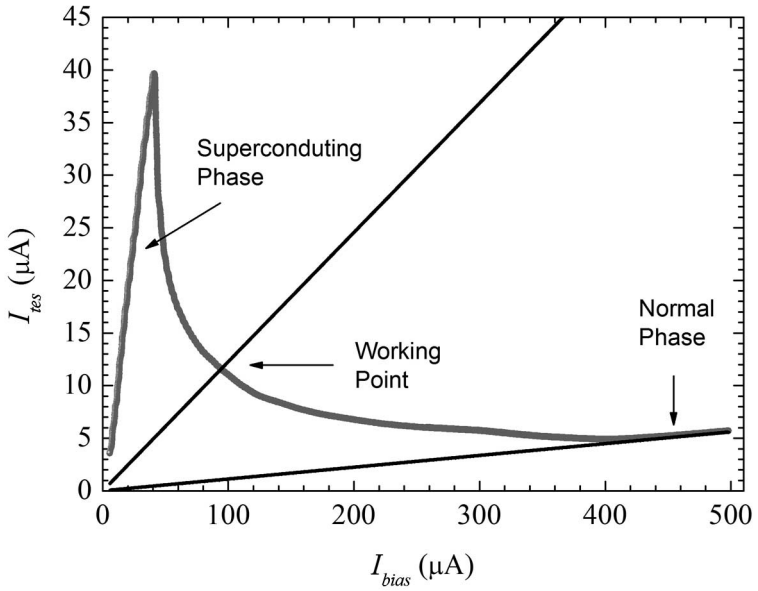

Fig. 2. – TES bias curve I_{tes} *vs.* I_{bias}. The black straight lines indicate the 17 mΩ resistance corresponding to the working point into the transition region and the 220 mΩ resistance of the normal phase.

have been acquired, from 2 Hz to 250 kHz, for different bias points (different % of R_N) and rappresented in the complex plane (solid dots) as shown in fig. 3 with the corresponding fit curves (lines). All the points have been normalized with respect to the actual fitted value of β since at high frequencies the real part of the impedance is given by $\mathrm{Re}[\mathrm{Z}(f)] = R_{sh} + R_0(1+\beta)$. In this fit analysis, the thermal conductance G has been shared by the multiple curves involved during the fit in order to obtain a robust parameter estimation [11]. The G value obtained is 14 pW/K, while the other parameters vary through the transition (from 20% to 80% of R_N), C from 1 to 0.3 fJ/K, α from 28 to 2 and β from 2.7 to 0.2. These values are comparable to those obtained for a similar TiAu TES in the corresponding bias point presented in a recent work [11].

3. – Photon counting

Four TESs are deposited on each SiN substrate (the TES chip carrier): two 20 μm × 20 μm and two 10 μm × 10 μm. To irradiate TESs we use a coupling system [6] that consists of an array of eight single-mode fibers, assembled on Si groove, glued to a copper bracket soldered to the TES chip carrier. The distance between two TESs with different area is the same between the first and the last fiber, so we can easily couple two detectors.

Illuminating the 20 μm × 20 μm detector with a pulsed diode laser at 690 nm (energy of single photon $E_\lambda = 1.80$ eV) with a pulse length of 0.1 μs, a repetition rate of 10 kHz and attenuating the light by neutral density filters, we obtain the histogram of the pulse amplitudes shown in fig. 4. The histogram has been processed by using a fit equation composed by a Gaussian function for each peak, with amplitude convoluted

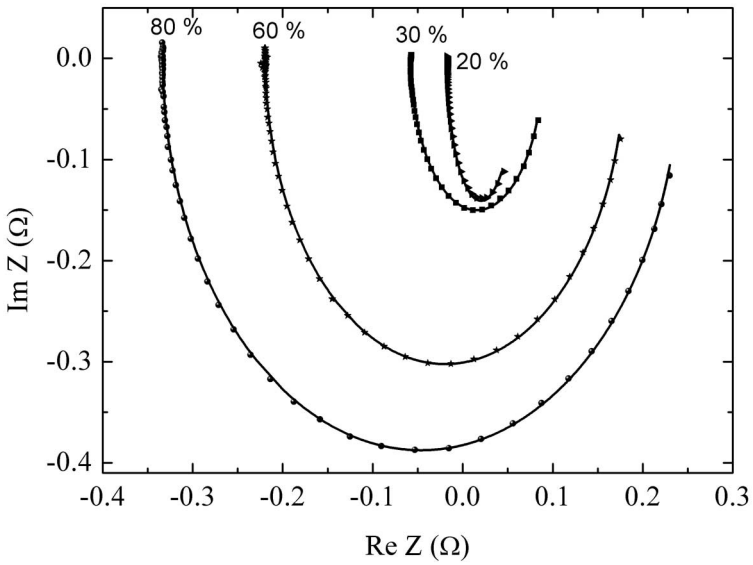

Fig. 3. – Representation of the experimental impedance data (solid dots) and the corresponding fit curves (lines) in the complex plane. The curves at different bias points have been normalized with respect to the actual fitted value of β. At high frequencies, the real part of the impedance is given by $\mathrm{Re}[\mathrm{Z}(f)] = R_{sh} + R_0(1+\beta)$.

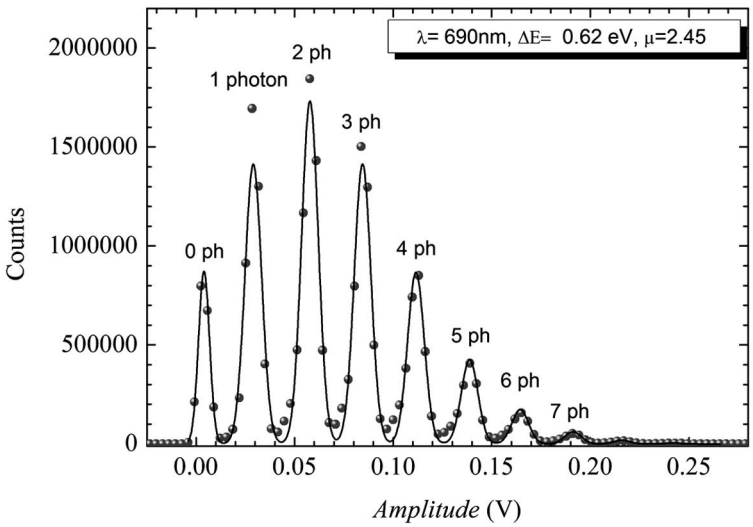

Fig. 4. – Histogram of the pulse amplitudes where up to 7 absorbed photons can be discriminated at 690 nm, by our $20\,\mu\mathrm{m} \times 20\,\mu\mathrm{m}$ TES with an energy resolution $\Delta E = 0.62\,\mathrm{eV}$ and averaged number of photons per pulse $\mu = 2.45$.

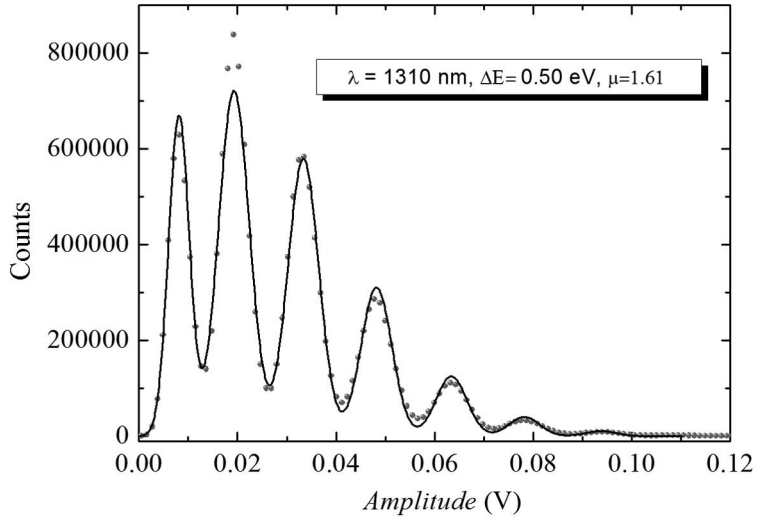

Fig. 5. – Histogram of the pulse amplitudes where up to 6 absorbed photons can be discriminated at 1310 nm, by our $20\,\mu\text{m} \times 20\,\mu\text{m}$ TES. The energy resolution is $\Delta E = 0.50\,\text{eV}$ and the averaged number of photons per pulse is $\mu = 1.61$.

with a Poissonian function [12]. In this way, for the results presented in fig. 4, we obtain an averaged number of absorbed photons per pulse $\mu = 2.45$ and a full width at half maximum energy resolution $\Delta E = 0.62\,\text{eV}$.

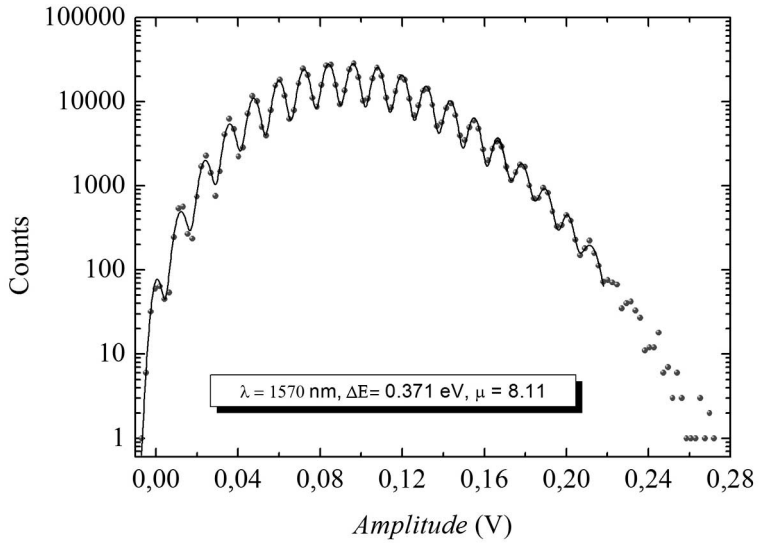

Fig. 6. – Histogram, in logarithmic scale, where up to 18 absorbed photons are discriminated at 1570 nm, with an energy resolution $\Delta E = 0.37\,\text{eV}$ and averaged number of photons per pulse $\mu = 8.11$.

Irradiating the same TES with a 80 ns pulsed laser source at 1310 nm ($E_\lambda = 0.95\,\text{eV}$), with a repetition rate of 10 kHz, we obtain the result shown in the histogram of fig. 5. The fit result, as previously described, gives an averaged number of absorbed photons per pulse $\mu = 1.61$ and a full width at half maximum energy resolution $\Delta E = 0.50\,\text{eV}$.

For a wider optical characterization of our detector, we irradiated the TES by using also an attenuated diode laser at 1570 nm ($E_\lambda = 0.79\,\text{eV}$), with a pulse length of 70 ns and 9 kHz of repetition rate. As shown in logarithmic scale in fig. 6, in this case we used a higher level of light intensity and we are able to discriminate up to 18 absorbed photons per pulse ($\mu = 8.11$), with an energy resolution of $\Delta E = 0.371\,\text{eV}$.

4. – Conclusion

In this work the results obtained at INRIM with TESs superconducting single-photon detectors in the visible-NIR wavelength range are reported. TESs are worldwide considered today the best available photon-number–resolving detectors. They are foundamental for the new quantum technologies and for single-photon metrology.

A $20\,\mu\text{m} \times 20\,\mu\text{m}$ TiAu TESs has been characterized with the complex impedance method and single photon counting experiments have been performed at 690 nm, 1310 nm and 1570 nm. The best measured energy resolution is $\Delta E = 0.37\,\text{eV}$ at 1570 nm and up to 18 photons have been discriminated in a single light pulse.

* * *

This work has been supported in part by the European Community Seventh Framework Programme, ERA-NET Plus, under Grant Agreement No. 217257.

REFERENCES

[1] Hadfield R. H., *Nat. Photon*, **3** (2009) 696.
[2] `www.quantumcandela.net`.
[3] Brida G., Genovese M. and Gramegna M., *Laser Phys. Lett.*, **3** (2006) 115.
[4] Rajteri M., Taralli E., Portesi C. and Monticone E., *Nuovo Cimento C*, **31** (2008) 549.
[5] Taralli E., Portesi C., Lolli L., Monticone E., Rajteri M., Novikov I. and Beyer J., *Supercond. Sci. Technol.*, **23** (2010) 105012.
[6] Lolli L., Taralli E., Portesi C., Alberto D., Rajteri M. and Monticone E., *IEEE Trans. Appl. Supercond.*, **21** (2011) 215.
[7] Portesi C., Taralli E., Rocci R., Rajteri M. and Monticone E., *J. Low Temp. Phys.*, **151** (2008) 261.
[8] Drung D., *IEEE Trans. Appl. Supercond.*, **17** (2007) 699.
[9] Irwin K. D., *Appl. Phys. Lett.*, **66** (1995) 1998.
[10] Lindeman M. A., Bandler S., Brekosky R. P., Chervenak J. A., Feliciano E. F., Finkbeiner F. M., Li M. J. and Kilbourne C. A., *Rev. Sci. Instrum.*, **75** (2004) 1283.
[11] Taralli E., Portesi C., Lolli L., Rajteri M. and Monticone E., submitted to *Eur. Phys. J. Plus*.
[12] Lolli L., Brida G., Degiovanni I. P., Genovese M., Gramegna M., Monticone E., Piacentini F., Portesi C., Rajteri M., Taralli E., and Traina P., *Int. J. Quantum Inf.*, **9** (2011) 405.